



New insights into the environmental drivers of the circumpolar ground thermal regime

Olli Karjalainen¹, Miska Luoto², Juha Aalto^{2,3}, and Jan Hjort¹

¹Geography Research Unit, University of Oulu, FI-90014, Oulu, Finland

5 ²Department of Geosciences and Geography, University of Helsinki, FI-00014, Helsinki, Finland

³Finnish Meteorological Institute, FI-00101, Helsinki, Finland

Correspondence to: Olli Karjalainen (olli.karjalainen@oulu.fi)

10 **Abstract.** The thermal dynamics of permafrost shape Earth surface systems and human activity in the Arctic and have implications to global climate. Improved understanding of the fine-scale variability in the circumpolar ground thermal regime is required to account for its sensitivity to changing climatic and geocological conditions. Here, we statistically related circumpolar observations of mean annual ground temperature (MAGT) and active-layer thickness (ALT) to high-resolution (~1 km²) geospatial data to identify their key environmental drivers. The multivariate models fitted well to MAGT and ALT observations with average R² values being ~0.94 and 0.78, respectively. Corresponding predictive performances in terms of root mean square error were ~1.31 °C and 87 cm. Freezing air temperatures were the main driver of MAGT in permafrost conditions while thawing temperatures dominated when permafrost was not present. ALT was most strongly related to solar radiation and precipitation with an important influence from soil properties. Our findings suggest that in addition to climatic factors, initial ground thermal conditions and local-scale topography-soil-driven variability need to be considered in order to realistically assess the impacts of climate change on cold-climate geoccosystems.

20 1 Introduction

In the face of changing Arctic, it is crucial to understand the mechanisms that drive the current geocryological development of the region. Thaw of permafrost is expected to significantly attribute to hydrological and geocological alterations in landscapes (Jorgenson et al., 2013; Liljedahl et al., 2016). In addition, greenhouse gas emissions from thawing permafrost soils have a potential to affect the global climate system (e.g. Grosse et al., 2016). Permafrost temperature and the depth of the overlying seasonally thawed layer, i.e. active layer, are key components of the ground thermal regime that govern various geomorphological and ecological processes (Frauenfeld et al., 2007; Aalto et al., 2017), as well as human activity in permafrost regions (Callaghan et al., 2011; Vincent et al., 2017). Outside the permafrost domain, extensive regions undergo seasonal freezing, which in itself affects many aspects of natural and human activity (e.g. Shiklomanov, 2012; Westermann et al., 2015).

30 Air temperature and precipitation account for large-scale spatial variation in mean annual ground temperature (MAGT) and active-layer thickness (ALT) (Bonnaventure and Lamoureux, 2013; Streletskiy et al., 2015; Westermann et al., 2015). From regional to local scales, topography-induced solar radiation input (Etzelmüller, 2013) and intercepting layers of soil, vegetation and snow mediate their effect (e.g. Osterkamp, 2007; Fisher et al., 2016; Gruber et al., 2017; Aalto et al., 2018a; Zhang et al., 2018). Winter temperatures have been suggested to be most important for permafrost temperature (Smith and Riseborough, 1996; Etzelmüller et al., 2011), while ALT is essentially dependent on summer temperatures (Oelke et al., 2003; Melnikov et al., 2004; Luo et al., 2016). In wintertime, snow layer insulates the ground from cold air causing an offset, i.e. ground temperatures are higher than air (e.g. Aalto et al., 2018b; Zhang et al., 2018). Water precipitation alters the thermal conductivity of near-surface layers through its control on, e.g., soil water balance (Smith and Riseborough, 1996; Callaghan et al., 2011; Marmy et al., 2013). Arguably, the responsiveness of the circumpolar ground thermal regime to atmospheric forcing also



40 depends on its initial thermal state. In permafrost conditions, temperature changes are lagged by the higher demand of energy
for phase changes of water in the active layer (i.e. latent-heat exchange), whereas in temperate soils climate signal affects more
directly (Kurylyk et al., 2014; Ekici et al., 2015).

Improved knowledge on permafrost dynamics is required to understand various geocological interactions and feedbacks
associated with warming Arctic (e.g. Wu et al., 2012; Grosse et al., 2016; Yi et al., 2018). Such information is useful for
climate change assessments (Zhang et al., 2005, Smith et al., 2009), infrastructure design and maintenance, as well as for
45 adaptation to changing conditions (Romanovsky et al., 2010, Streletskiy et al., 2015). Despite the increased availability of
MAGT and ALT measurements (Biskaborn et al., 2015) and global geospatial data, fine-scale analyses of the environmental
drivers over the circumpolar area are largely lacking. Physically based ground thermal models can account for various
biogeophysical processes acting in vegetation, snow and soil layers (e.g. Lawrence and Swenson, 2011) but are not applicable
at fine spatial resolutions for large areas owing to their tedious model parameterizations (Chadburn et al., 2017). For example,
50 commonly used circumpolar 0.5° latitude/longitude resolution has been considered insufficient in characterizing spatial
variation in soil properties and vegetation, thus leading to large mismatch between the simulations and observations (Park et
al., 2013). Peng et al. (2018) assessed long-term trends in circumpolar ALT with a large observational dataset stressing that
ALT strongly depends on local topo-edaphic factors and that thorough analyses of environmental factors controlling ALT are
urgently required.

55 Here, we use a statistical modelling framework employing multiple algorithms from regression to machine learning to examine
the drivers controlling the spatial variation in the circumpolar ground thermal regime. More specifically, we aim to (1) calibrate
realistic models of MAGT and ALT (the responses) utilizing geospatial data on climatic and local conditions (the predictors),
and (2) assess the relative contribution of the drivers in both permafrost and non-permafrost conditions using geographically
comprehensive datasets of field-quantified MAGT (n = 784) and ALT (n = 298) observations.

60 2 Methods

2.1 Study area and observational data

We compiled MAGT and ALT observations from the period 2000–2014 over the Northern Hemisphere land areas north of the
30th parallel (Fig.1). To examine possible variation in the contribution of environmental factors between permafrost and non-
permafrost conditions we used two separate MAGT datasets; observed MAGT at or below 0 °C, i.e. permafrost, (MAGT_{≤0} °C,
65 n = 469) and above 0 °C (MAGT_{>0} °C, n = 315). The observations were standardized by requiring that MAGT was recorded
at or near the depth of zero annual amplitude (ZAA) where annual temperature variation was less than 0.1 °C, and that ALT
was measured at the end of thawing season during the maximum thaw (Brown et al., 2000; Aalto et al., 2018a). When ZAA
depth was not reported or not retrievable from numeric data, we used the value at the depth of 15 m, where annual temperature
fluctuation is negligible (see French, 2007). With some MAGT observations, ZAA depth was reportedly not reached but we
70 chose to include these cases assuming that annual means calculated from year-round records from one or multiple years were
representative of long-term thermal state. MAGT values shallower than two meters below the surface were systematically
excluded unless reported to be at the depth of ZAA.

The Global Terrestrial Network for Permafrost database (GTN-P, Biskaborn et al., 2015) was the principal constituent of our
datasets (~60 % of MAGT and ~67 % of ALT observations). Additionally, data were gathered from open Internet databases
75 (e.g. Roshydromet, meteo.ru; Natural Resources Canada, GEOSCAN database; National Geothermal Data System) and
previous studies to cover a maximal range of climatological and environmental conditions (see Table S1 and S2 for sources)



80 A minimum geospatial location precisions of two decimal degrees (~1,110 m at the Equator) for MAGT and a commonly used arc minute (~1,800 m) for often less accurately geospatially positioned ALT sites were adopted both to ascertain adequate spatial match with geospatial data layers and to moderate the need to exclude lower precision observations. Nonetheless, almost 90 % of MAGT and more than two-thirds of ALT observations had a precision of at least three decimal degrees (~110 m at the Equator). Further exclusions were made when the ground thermal regime was evidently disturbed by recent forest fire, anthropogenic heat source, large water bodies or the effect of geothermal heat in temperature-depth curve (Jorgenson et al., 2010; Woo, 2012) as revealed by source data or cartographical examination of the site.

2.2 Predictor variables

85 Nine geospatial predictors presenting climatic (air temperature and precipitation) and local (potential incident solar radiation, vegetation and soil properties) conditions at 30 arc-second spatial resolution were selected to examine their potential effects on MAGT and ALT (e.g. Brown et al., 2000; French, 2007; Jorgenson et al., 2010; Bonnaventure & Lamoureux, 2013; Streletskiy et al., 2015). Climatic parameters were derived from the WorldClim dataset (Hijmans et al., 2005). The temporal coverage of WorldClim is 1950–2000, so we adjusted the data to match our study period of 2000–2014 using the Global Meteorological Forcing Dataset for land surface modelling (GMFD, Version 2, Sheffield et al., 2006) at a 0.5-degree resolution
90 (see Aalto et al., 2018a).

Previous studies have suggested that using indices representing the length or magnitude of thawing and freezing season could be more suitable than annual mean of air temperature (e.g. Zhang et al., 1997; Smith et al., 2009). Thus, thawing (TDD) and freezing (FDD) degree-days were determined as cumulative sums of mean monthly air temperatures above and below 0 °C,
95 respectively (Frauenfeld et al., 2007). Since available global data on snow thickness or snow-water equivalency have relatively coarse spatial resolutions (Bokhorst et al., 2016), we examined the snow cover's contribution indirectly using derivatives of the climate data. We estimated annual snow and rainfall by summing up precipitation (mm) for months with mean monthly temperature below and above 0 °C, respectively (Zhang et al., 2003).

100 MODIS Terra-based normalized difference vegetation indices (NDVI, Didan, 2015) at a 1-km resolution were used to assess the amount of photosynthetic vegetation. We averaged monthly summertime (June to August) NDVI values over the study period of 2000–2014 and screened for only high-quality pixels based on the MODIS pixel reliability attribute. Potential incident solar radiation, computed after McCune and Keon (2002, Equation 2, p. 605) utilizing slope angle and aspect, along with latitude, was used to estimate the potential incident solar radiation (PISR) that affects the energy balance of the ground thermal regime (e.g. Hasler et al., 2015; Streletskiy et al., 2015). Soil organic carbon content (SOC, g kg⁻¹), and fractions of
105 coarse (CoarseSed, > 2 mm) and fine sediments (FineSed, ≤ 50 µm) for 0–200 cm subsurface, were extracted from SoilGrids database (Hengl et al., 2017).

2.3 Statistical modelling

2.3.1 Calibration of MAGT and ALT models

110 We used four statistical techniques, namely generalized linear modelling (GLM, McCullagh and Nelder, 1989), generalized additive modelling (GAM, Hastie and Tibshirani, 1990), and regression-tree based machine-learning methods generalized boosting method (GBM, Friedman et al., 2000) and random forest (RF, Breiman 2001) to calibrate MAGT and ALT models by using the nine geospatial predictors. Multi-model framework was adopted to control for uncertainties related to the choice of modeling algorithm (e.g. Heikkinen et al., 2006). GLM is an extension of linear regression capable of handling non-linear relationships with an adjustable link function between the response and explanatory variables. The GLM models were fitted
115 including quadratic terms for each predictor. In GAM, alongside linear and polynomial terms, smoothing splines can be applied



for more flexible handling of non-linear relationships. For smoothing spline, a maximum of three degrees of freedom were specified, which was further optimized by the model fitting function. To examine the direction and possible non-linearity of the relationship between predictors and responses, we used GAM to plot model-based univariate response curves. Both GLM and GAM were fitted without interactions between predictors using a Gaussian error distribution with an identity link function.

120 GBM was specified with the following parameters: number of trees = 3,000, interaction depth = 6, shrinkage = 0.001. Bagging fraction was set to 0.75 to select a random subset of 75 % of the observations at each step, without replacement. As for RF, 500 trees, each with a minimum node size of five were grown. The final prediction is the average of individual tree predictions. Both GBM and RF automatically consider interaction effects between predictors (Friedman et al., 2000). All statistical analyses were executed in R (R Core team, 2015) using auxiliary R packages; *mgcv* (Wood, 2011) for GAM, *dismo* (Hijmans et al., 2016) for GBM, and *randomForest* for RF (Liaw and Wiener, 2002).

125

2.3.2 Model evaluation

To evaluate the models, we split the response data randomly into calibration (70 % of the observations) and evaluation (30 %) datasets (Heikkinen et al., 2006). This was repeated 100 times, at each step fitting models with the calibration data and then using them to predict to both the calibration and evaluation datasets. Model performance was assessed with adjusted coefficient of determination (R^2) and root mean square error (RMSE) between observed and predicted values in these datasets.

130

2.3.3 Variable importance computation

A measure of variable importance was computed to determine the relative importance of each predictor to the models' predictive performance (Breiman, 2001). In the computation, each modelling technique was first used to fit models with the MAGT and ALT datasets using all the nine predictors. The variable importance was then computed based on Pearson's correlation between predictions from two models produced with the fitted model; one with unchanged variables, and another where the values of one variable were randomized while others remained intact (Breiman, 2001). In the procedure, each predictor was randomized in successive model runs. The measure of variable importance was computed as follows:

135

$$\text{Variable importance} = 1 - \text{corr}(\text{Prediction}_{\text{intact variables}}, \text{Prediction}_{\text{one variable randomized}}) \quad (1)$$

On a range from 0 to 1, high variable importance value, i.e. high individual contribution to MAGT or ALT, was returned when any randomized predictor had a substantial impact on the model's predictive performance, and consequently resulted low correlation with predictions from the model with intact variables (Thuiller et al., 2009). Each modelling method was run 100 times for each response with each predictor shuffled separately. For each run, different subsample from the original data was randomly bootstrapped with replacement.

140

2.3.4 Effect size statistics

Effect sizes for each predictor were determined based on the range between the predicted minimum and maximum MAGT and ALT values over the observation data while controlling for the influence of other predictors by fixing them at their mean values (see Nakagawa and Cuthill, 2007). The procedure was repeated with each dataset and modelling method.

145

3 Results

MAGT in permafrost conditions was on average -3.1 °C while the minimum was -15.5 °C. $\text{MAGT}_{>0$ °C had an average of 8.0 °C and a maximum of 23.2 °C. ALT had an average of 141 cm and ranged from 23 to 733 cm. The extreme values, apart from the ALT maximum, were based on one year of measurements. Pairwise correlations and the scatter plots revealed a strong

150



association between MAGT and air temperature, especially in $MAGT_{>0\text{ }^{\circ}\text{C}}$ (Fig. 2a–b, d). In contrast to MAGT, ALT was not significantly correlated with TDD, but had stronger associations with soil properties (Fig. 2c). Statistical descriptives of the predictors in respective datasets are presented with box-plots (Fig. S1).

155 3.1 Model performance

$MAGT_{>0\text{ }^{\circ}\text{C}}$ models had the highest R^2 values between predicted and observed MAGT (Table 1). In permafrost conditions, all the models had high R^2 values for MAGT, whereas in case of ALT between-model variation was large and R^2 on average lower. A decrease in the fit was identified when predicting ALT to evaluation datasets, especially with GBM and RF, whereas MAGT models retained their high performance. According to changes in RMSE between calibration and evaluation datasets, 160 GLM and GAM produced more accurate predictions than GBM and RF for each response.

3.2 Relative importance of individual variables

FDD and TDD were the most important drivers of MAGT; FDD (0.27) where permafrost was present, TDD (0.53) in non-permafrost conditions (Fig. 3a–b). Precipitation predictors, especially water precipitation, had a moderate importance (0.10) on $MAGT_{\leq 0\text{ }^{\circ}\text{C}}$ but were marginal when permafrost was not present (0.01). Climatic drivers were followed by solar radiation 165 (0.02, both MAGT datasets) and finally by NDVI and soil properties with minimal importance (each ≤ 0.01). The importance of both water and snow precipitation was higher in permafrost conditions.

Solar radiation was the most important predictor (0.37) explaining variation in ALT (Fig. 3c). Water precipitation had second highest importance (0.05) followed by soil properties SOC (0.04) and coarse sediments (0.03). The remaining climate variables (snow precipitation, TDD and FDD) had low importance scores that were comparable to those of NDVI (each 0.01–0.02).

170 3.3 Effect size of individual variables

FDD had the highest individual effect size of $6.7\text{ }^{\circ}\text{C}$ averaged over the four methods in case of $MAGT_{\leq 0\text{ }^{\circ}\text{C}}$, whereas in $MAGT_{>0\text{ }^{\circ}\text{C}}$ dataset TDD accounted for a dominant $13.6\text{ }^{\circ}\text{C}$ effect (Table 2). Precipitation had the next highest effect, albeit snow precipitation was less effective in non-permafrost conditions. In case of ALT, water precipitation exerted the greatest effect (181 cm) despite large between-model variation. Solar radiation had a central role with a highly non-linear shape of response 175 (Fig. 4c). A varying degree of non-linearity is visible in the responses between $MAGT_{\leq 0\text{ }^{\circ}\text{C}}$ and the key predictors, whereas in case of $MAGT_{>0\text{ }^{\circ}\text{C}}$ the responses are more linear (Fig. 4a–b).

4 Discussion

4.1 Circumpolar drivers of MAGT and ALT

Our results show that climatic conditions are the primary drivers of long-term averages of circumpolar MAGT but also indicate 180 that the effects of TDD and FDD are dependent on initial ground thermal conditions. FDD has higher influence on MAGT in permafrost conditions where strong freezing leads to negative surface energy balance and occurrence of permafrost (e.g. Smith & Riseborough, 1996). At sites without permafrost, TDD has the dominant effect, which is suggested to be mostly attributed to the lack of the buffering effect of the freeze-thaw processes and latent-heat exchange in the active layer (e.g. Osterkamp, 2007), and to the absence of seasonal or permanent snow cover in the warmest parts of the study region. In permafrost 185 conditions, the warming effect of TDD and especially the cooling effect of FDD on MAGT show flattening in response shapes where MAGT is close to $0\text{ }^{\circ}\text{C}$ owing to the latent-heat effects associated with thawing and freezing of water in the active layer (Fig. 4a).



190 The minimal effect of TDD on ALT contradicts with the documented strong regional scale (spatio)temporal connection (e.g. Zhang et al., 1997; Oelke et al., 2003; Frauenfeld et al., 2004; Melnikov et al., 2004; Yi et al., 2018). According to our results, the spatial linkage is more elusive at a broader scale and could be attributed to the great circumpolar variation in ALT; high-Arctic sites have decimeter thaw depths, while ALT in similar average climatic conditions can be several meters in mountainous areas (e.g. Bonnaventure and Lamoureux, 2013; Luo et al., 2016). Moreover, large inconsistencies between observed ALT and climate-warming trends have been documented (e.g. Wu et al., 2012; Gangodagamage et al., 2014).

195 Recent warming trends in the atmosphere (Guo et al., 2017) are already well visible in circumpolar permafrost temperature observations (Romanovsky et al., 2017) implying that the permafrost system will remain dynamic in future's changing climate. Warmer air temperatures will occur mostly during winters (AMAP, 2017; Guo et al., 2017), which, given the presented high contribution of FDD on MAGT, suggests that changes are foreseeable. Projected warmer winters can also affect ALT through changing snow conditions and subsequent changes in hydrology and vegetation (Park et al., 2013; Atchley et al., 2016; Peng et al., 2018).

200 According to Kurylyk et al. (2014), permafrost studies often consider only conductive heat propagation in the ground. Vincent et al. (2017), however, stress the need to acknowledge processes associated with liquid water and advective heat in efforts to understand rapidly changing cryosphere. In line with new studies (Peng et al., 2018; Zhang et al., 2018), our results highlight the notable role of water precipitation on both MAGT and ALT. Projected greater proportion of liquid precipitation (e.g. AMAP, 2017; Bintanja and Andry, 2017) potentially has a direct effect on the ground thermal regime through convective warming during spring (Kane et al., 2001) and summertime (Melnikov et al., 2004; Marmy et al., 2013). However, abundant summer rains arguably also cool the ground surface through increased evaporation and heat capacity, and thus limit the heat conduction into the ground (Zhang et al., 1997, 2005; Frauenfeld et al., 2004; Park et al., 2013). Moreover, extreme climatic events, such as wintertime rain events can have a distinct effect on soil temperature (Westermann et al., 2011) although the long-term sensitivity of permafrost to them is not fully clear yet (Marmy et al., 2013).

210 The dominant contribution of water precipitation over snowfall observed here contradicts with some previous regional scale studies (e.g., Zhang et al., 2003, 2005). However, the elevated effect of snowfall on MAGT in permafrost conditions (2.3 °C compared to 0.8 °C in non-permafrost conditions) underlines the role of snow cover's control over the ground thermal regime. Similarly, Zhang et al. (2018) found that the offset between air and surface temperatures was weaker in temperate regions (mean annual air temperature >0 °C) than in low-Arctic and boreal permafrost regions, although also high-Arctic had small offsets owing to small amount of snow. Despite the complexity involved in snow's role (e.g. Fiddes et al., 2015; Aalto et al., 2018b), thick snow cover has been shown to increase also ALT at site (Atchley et al., 2016), regional (Zhang et al., 1997; Frauenfeld et al., 2004) and circumpolar scale (Park et al., 2013).

220 Incoming solar energy can be considered central for soil thawing (see Biskaborn et al., 2015), but the high contribution of solar radiation on ALT stands out as well. Arguably, the effect is emphasized because ALT observation sites in cold permafrost conditions are mostly sparse in vegetation and lack tree canopy (Zhang et al., 2003; Biskaborn et al., 2015). Moreover, most of the ALT sites have been established on flat terrain (Biskaborn et al., 2015), meaning that local topographic shading is less significant. Thus, ALT is suggested to follow poleward decrease in solar radiation and associated shorter thaw seasons (see Luo et al., 2016). The weaker association of solar radiation with MAGT suggests that its direct effect is limited to the near-surface permafrost, i.e. intensified thawing during thawing seasons, and that the influence to deeper temperatures is more indirect and associated with the relationship between annual solar radiation and air temperatures.

225 The weak connection between TDD and ALT is additionally explained by soil factors that influence the heat transfer between the lower atmosphere and the ground (Smith et al., 2009). According to the response shapes from GAM, coarse sediments



230 increase ALT when enough prevalent (~25 % fraction) in the soils. The effect of soil texture on ALT has been implied to occur
largely through its effects on hydrological conditions (Zhang et al., 2003; Yin et al., 2017) and conductivity (Callaghan et al.,
2011). More efficient water transfer in coarse-grained material could impose convective heat into soils during the thawing
season or promote latent-heat effect during the freeze-up, which both contribute to deeper thaw (see Romanovsky and
Osterkamp, 2000; Frauenfeld et al., 2004). Insulation by soil organic layers has been demonstrated to effectively decouple air-
permafrost connection resulting in thinner active layer and lower soil temperatures (e.g. Johnson et al., 2013; Atchley et al.,
2016). The GAM response shape illustrates a thinning of ALT with increasing SOC until ~150 g kg⁻¹, after which additional
235 organic material does not attribute to enhanced insulation.

NDVI has a small contribution on ALT and MAGT in permafrost conditions, but outside the permafrost region it has a
moderate cooling effect. The low contribution of NDVI in permafrost conditions could be attributed to the intra- and inter-
seasonal differences in the effects of vegetation. In wintertime, low vegetation traps snow and thereby enhances insulation of
the ground. Taller tree canopies of evergreen boreal forests, in turn, intercept snow and allow more heat loss from the ground
240 in winter, while in summer their shading cools the ground surface (Lawrence and Swenson, 2011; Fisher et al., 2016).

4.2 Uncertainties

Large-scale scrutinization of factors affecting ground thermal dynamics is often hindered by data deficiencies or unavailability.
More precisely, many data lack adequate spatial or temporal accuracy, geographical consistency, methodological robustness
or thematic detail (Bartsch et al., 2016; Chadburn et al., 2017). Some of these shortcomings are exacerbated in remote
245 permafrost regions with low-density observational networks of, e.g., climatic parameters (Hijmans et al., 2005) or soil profiles
(Hengl et al., 2017). The fine-scale spatial variability of ALT and MAGT called for a high spatial resolution data to assess the
local factors that mediate the atmospheric forcing. Here, the availability of geospatial data largely determined the resolution
of 30 arc seconds, which could be considered the highest currently attainable resolution at a near-global scale. While not
adequate to account for all potential sources of sub-grid spatial heterogeneity in, e.g. microclimatic conditions, especially in
250 topographically complex conditions (Fiddes et al., 2015; Aalto et al., 2018b; Yi et al., 2018), the implemented resolution is a
step forward in making a distinction in between-site conditions and revealing local relationships relevant at the circumpolar
scale.

In general, the sensitivity of MAGT to the climatic parameters along with the minimal role of soil and vegetation properties
suggests that circumpolar future predictions of MAGT are more applicable than those of ALT, even without addressing, for
255 example, future vegetation or soil organic carbon content, whose response to climate change is extremely challenging to project
(Jorgenson et al., 2013). Given the pronounced role of precipitation, more direct information on fine-scale soil moisture
conditions controlled by local soil and land surface properties (see Kempinen et al., 2018), as well as more comprehensive
and finer resolution data on circumpolar snow thickness are required for improved ground thermal regime modelling.

Although the main drivers were identified as important and effective by each modelling technique, notable inter-modal
260 variability suggested that using only one method could have led to disputable results. A multi-model approach was in this
sense safer, although not all the methods may have worked optimally with the present observational and environmental data
owing to their different abilities to handle collinearity, spatial autocorrelation or non-linearity. For example, interactions
between variables were not included in regression-based modelling (GLM and GAM), while being intrinsically considered by
tree-based methods (GBM and RF) (Friedman et al., 2000). Differences such as this could have attributed to the dissimilar
265 performances of the models; GBM and RF were overall less stable when comparing R² and RMSE values between the observed
and predicted values in calibration and evaluation settings.



5 Conclusions

We assessed the drivers of the circumpolar ground thermal regime at an unprecedentedly fine 1-km spatial resolution using comprehensive field-quantified observational datasets. Our statistical modelling framework efficiently captured the multi-variate nature of MAGT and ALT and highlighted the difference between the contributions of climatic factors on MAGT inside and outside the permafrost domain. The findings imply that, in addition to reliably addressing the key climatic factors, realistic future climate change assessments of Earth surface systems should take into account initial ground thermal conditions. Furthermore, the thermal state of permafrost in terms of MAGT and ALT was controlled by distinctive factors. Although of little importance for MAGT, soil properties had a momentous effect on ALT and should thus be accounted for in simulations of permafrost thaw. In addition to providing theoretical insights, multi-variate modelling frameworks capable of employing global geospatial data at fine spatial resolution, are valuable for the Arctic research, e.g. greenhouse gas emissions from thawing permafrost soils.

Author contribution

OK, ML and JH developed the original idea. OK led the compilation of observational data and geospatial data processing with contributions from all the authors. ML, OK and JA performed the statistical analyses. OK wrote the manuscript with contributions from all the authors.

Acknowledgements. This study was funded by the Academy of Finland (grants 285040 and 286950).

Competing interests

The authors declare that they have no conflict of interest.

References

- Aalto, J., Harrison, S., and Luoto, M.: Statistical modelling predicts almost complete loss of major periglacial processes in Northern Europe by 2100, *Nat. Comm.*, 8, doi.org/10.1038/s41467-017-00669-3, 2017.
- Aalto, J., Karjalainen, O., Hjort, J., and Luoto, M.: Statistical Forecasting of Current and Future Circum- Arctic Ground Temperatures and Active Layer Thickness, *Geophys. Res. Lett.*, 45, doi.org/10.1029/2018GL078007, 2018a.
- Aalto, J., Scherrer, D., Lenoir, J., Guisan, A., and Luoto, M.: Biogeophysical controls on soil-atmosphere thermal differences: implications on warming Arctic ecosystems, *Environ. Res. Lett.*, in press, doi.org/10.1088/1748-9326/aac83e, 2018b.
- AMAP: Snow, Water, Ice and Permafrost in the Arctic (SWIPA): Climate Change and the Cryosphere, Arctic Monitoring and Assessment Programme (AMAP), Oslo, Norway, 2017.
- Atchley, A. L., Coon, E. T., Painter, S. L., Harp, D. R., and Wilson, C. J.: Influences and interactions of inundation, peat, and snow on active layer thickness, *Geophys. Res. Lett.*, 43, 5116–5123, [doi:10.1002/2016GL068550](https://doi.org/10.1002/2016GL068550), 2016.
- Bartsch, A., Höfler, A., Kroisleitner, C., and Trofaier, A. M.: Land cover mapping in northern high latitude permafrost regions with satellite data: achievements and remaining challenges, *Remote Sens.*, 8, 979, [doi:10.3390/rs8120979](https://doi.org/10.3390/rs8120979), 2016.
- Bintanja, R. and Andry, O.: Towards a rain-dominated Arctic. *Nat. Clim. Change*, 7, 263–267, [doi: 10.1038/nclimate3240](https://doi.org/10.1038/nclimate3240), 2017.
- Biskaborn, B. K., Lanckman, J.-P., Lantuit, H., Elger, K., Streletskiy, D. A., Cable, W. L., and Romanovsky, V. E.: The new database of the Global Terrestrial Network for Permafrost (GTN-P), *Earth Syst. Sci. Data* 7, 245–259, 2015.



- Bokhorst, S., Højlund Pedersen, S., Brucker, L., Anisimov, O., Bjerke, J. W., Brown, R. D., Ehrich, D., Essery, R. L. H., Heilig, A., Ingvander, S., Johansson C., Johansson, M., Jónsdóttir, I. S., Inga, N., Luoju, K., Macelloni, G., Mariash, H., McLennan, D., Rosqvist, G. N., Sato, A., Savela, H., Schneebeli, M., Sokolov, A., Sokratov, S. A., Terzagio, S., Vikhamar-Schuler, D., Williamson, S., Qiu, Y., and Callaghan, T. V.: Changing Arctic snow cover: A review of recent developments and assessment of future needs for observations, modelling, and impacts, *Ambio*, 45, doi:10.1007/s13280-016-0770-0, 2016.
- Bonnaventure, P. P. and Lamoureux, S. F.: The active layer: A conceptual review of monitoring, modelling techniques and changes in a warming climate, *Prog. Phys. Geog.*, 37, 352–376, 2013.
- Breiman, L.: Random forests, *Machine Learning* 45, 5–32, 2001.
- Brown, J., Hinkel, K. M., and Nelson, F. E.: The circumpolar active layer monitoring (CALM) program: research designs and initial results, *Polar Geography*, 24, 165–258, 2000.
- Brown, J., Ferrians, O. J. Jr., Heginbottom, J. A., and Melnikov, E. S.: Circum-Arctic Map of Permafrost and Ground-Ice Conditions, Version 2, National Snow and Ice Data Center, <http://nsidc.org/data/ggd318>, 2002.
- Callaghan, T. V., Johansson, M., Anisimov, O., Christiansen, H. H., Instanes, A., Romanovsky, V. E., and Smith, S.: Changing permafrost and its impacts, in: *Snow, Water, Ice and Permafrost in the Arctic (SWIPA): Climate Change and the Cryosphere*, Arctic Monitoring and Assessment Programme (AMAP), Oslo, Norway, 2011.
- Chadburn, S. E., Burke, E. J., Cox, P. M., Friedlingstein, P., Hugelius, G., and Westermann, S.: An observation-based constraint on permafrost loss as a function of global warming, *Nature Climate Change*, 7, doi:10.1038/nclimate3262, 2017.
- Didan, K.: MOD13A2 MODIS/Terra Vegetation Indices 16-Day L3 Global 1km SIN Grid V006. NASA EOSDIS LP DAAC. doi: 10.5067/MODIS/MOD13A2.006, 2015.
- Ekici, A., Chadburn, S., Chaudhary, N., Hajdu, L. H., Marmy, A., Peng, S., Boike, J., Burke, E., Friend, A. D., Hauck, C., Krinner, G., Langer, M., Miller, P. A., and Beer, C.: Site-level model intercomparison of high latitude and high altitude soil thermal dynamics in tundra and barren landscapes, *The Cryosphere*, 9, 1343–1361, 2015.
- Etzelmüller, B.: Recent advances in mountain permafrost research, *Permafrost Periglac.*, 24, 99–107, 2013.
- Etzelmüller, B., Schuler, T. V., Isaksen, K., Christiansen, H. H., Farbro, H., and Benestad, R.: Modeling the temperature evolution of Svalbard permafrost during the 20th and 21st century, *The Cryosphere*, 5, 67–79, 2011.
- Fiddes, J., Endrizzi, S., and Gruber, S.: Large-area land surface simulations in heterogeneous terrain driven by global data sets: application to mountain permafrost, *The Cryosphere*, 9, 411–426, 2015.
- Fisher, J. P., Estop-Aragónés, C., Thierry, A., Charman, D. J., Wolfe, S. A., Hartley, I. P., Murton, J. B., Williams, M., and Phoenix, G. K.: The influence of vegetation and soil characteristics on active-layer thickness of permafrost soils in boreal forest, *Glob. Change Biol.*, 22, 3217–3140, 2016.
- Frauenfeld, O. W., Zhang, T., and Barry, R. G.: Interdecadal changes in seasonal freeze and thaw depths in Russia, *J. Geophys. Res.*, VOL. 109, D05101, doi:10.1029/2003JD004245, 2004.
- Frauenfeld, O. W., Zhang, T. and McCreight J. L.: Northern hemisphere freezing/thawing index variations over the twentieth century, *Int. J. Climatol.*, 27, 47–63, 2007.
- French, H. M.: *The Periglacial Environment*, 3rd Edn, Wiley, 2007.
- Friedman, J., Hastie, T., and Tibshirani, R.: Additive logistic regression: a statistical view of boosting, *The Annals of Statistics*, 28, 337–407, 2000.
- Gangodamage, C., Rowland, J. C., Hubbard, S. S., Brumby, S. P., Liljedahl, A. K., Wainwright, H., Wilson, C. J., Altmann, G. L., Dafflon, B., Peterson, J., Ulrich, C., Tweedie, C. E., and Wulschleger, S. D.: Extrapolating active layer



- thickness measurements across Arctic polygonal terrain using LiDAR and NDVI data sets, *Water Resources Research*, 50, 6339–6357, doi:10.1002/2013WR014283, 2014.
- 345 Grosse, G., Goetz, S., McGuire, A. D., Romanovsky, V. E. and Schuur, E. A. G.: Changing permafrost in a warming world and feedbacks to the Earth system, *Environ. Res. Lett.*, 11, 2016.
- Gruber, S., Fleiner, R., Guegan, E., Panday, P., Schmid, M.-O., Stumm, D., Wester, P., Zhang, Y., and Zhao, L.: Review article: Inferring permafrost and permafrost thaw in the mountains of the Hindu Kush Himalaya region, *The Cryosphere* 11, 81–99, 2017.
- 350 Guo, D., Li, D., and Hua, W.: Quantifying air temperature evolution in the permafrost region from 1901 to 2014, *Int. J. Climatol.*, 38, 66–76, doi: 10.1002/joc.5161, 2017.
- Hasler, A., Geertsema, M., Foord, V., Gruber, S., and Noetzi, J.: The influence of surface characteristics, topography and continentality on mountain permafrost in British Columbia, *The Cryosphere*, 9, 1025–1038, 2015.
- 355 Hastie, T. J. and Tibshirani, R. J.: *Generalized Additive Models*, CRC Press, 1990.
- Heikkinen, R. K., Luoto, M., Araújo, M. B., Virkkala, R., Thuiller, W., and Sykes, M. T.: Methods and uncertainties in bioclimatic envelope modelling under climate change, *Prog. Phys. Geog.*, 30, 751–777, 2006.
- Hengl, T., Mendes de Jesus, J., Heuvelink, G.B.M., Ruiperez Gonzalez, M., Kilibarda, M., Blagotić, A., Shangguan, W., Wright, M. N., Geng, X., Bauer-Marschallinger, B., Antonio Guevara, M., Vargas, R., MacMillan, R. A., Batjes, N.
- 360 H., Leenaars, J. G. B., Ribeiro, E., Wheeler, I., Mantel, S., and Kempen, B.: SoilGrids250m – Global gridded soil information based on machine learning, *PLoS ONE* 12, e0169748, doi.org/10.1371/journal.pone.0169748, 2017.
- Hijmans, R. J., Cameron, S. E., Parra, J. L., Jones, P. G., and Jarvis, A.: Very high resolution interpolated climate surfaces for global land areas, *Int. J. Climatol.*, 25, 1965–1978, 2005.
- Hijmans, R. J., Phillips S., Leathwick, J., and Elith, J.: *dismo: Species Distribution Modeling*. R package version 1.1-1. <http://cran.r-project.org/web/packages/dismo/index.html>, 2016.
- 365 Johnson, K. D., Harden, J. W., McGuire, A. D., Clark, M., Yuan, F., and Finley, A. O.: Permafrost and organic layer interactions over a climate gradient in a discontinuous permafrost zone, *Environ. Res. Lett.*, 8, 035028, 2013.
- Jorgenson, M. T., Romanovsky, V., Harden, J., Shur, Y., O'Donnell, J., Schuur, E. A. G., Kanevskiy, M., and Marchenko, S.: Resilience and vulnerability of permafrost to climate change, *Can. J. For. Res.*, 40, 1219–1236, 2010.
- 370 Jorgenson, M. T., Harden, J., Kanevskiy, M., O'Donnell, J., Wickland, K., Ewing, S., Manies, K., Zhuang, Q., Shur, Y., Striegl, R., and Koch, J.: Reorganization of vegetation, hydrology and soil carbon after permafrost degradation across heterogeneous boreal landscapes, *Environ. Res. Lett.*, 8, 035017, 2013.
- Kane, D. L., Hinkel, K. M., Goering, D. J., Hinzman, L. D., and Outcalt, S. I.: Non-conductive heat transfer associated with frozen soils, *Glob. Planet. Change*, 29, 275–292, 2001.
- 375 Kempainen, J., Niittynen, P., Riihimäki, H., and Luoto, M.: Modelling soil moisture in a high-latitude landscape using LiDAR and soil data, *Earth Surf. Process. Landforms*, 43, 1019–1031, doi: 10.1002/esp.4301, 2018.
- Kurylyk, B. L., MacQuarrie, K. T. B., and McKenzie, J. M.: Climate change impacts on groundwater and soil temperatures in cold and temperature regions: Implications, mathematical theory, and emerging simulation tools, *Earth-Sci. Rev.*, 138, 313–334, 2014.
- 380 Lawrence, D. M. and Swenson, S. C.: Permafrost response to increasing Arctic shrub abundance depends on the relative influence of shrubs on local soil cooling versus large-scale climate warming, *Environ. Res. Lett.*, 6, 045504, 2011.
- Liaw, A. and Wiener, M.: Classification and regression by randomForest, *R news* 2, 18–22, 2002.
- Liljedahl, A. K., Boike J., Daanen, R. P., Fedorov, A. N., Frost, G. V., Grosse, G., Hinzman, L. D., Iijma, Y., Jorgenson, J. C., Matveyeva, N., Necsoiu, M., Reynolds, M. K., Romanovsky, V. E., Schulla, J., Tape, K. D., Walker, D. A.,



- 385 Wilson, C. J., Yabuki, H. and Zona, D.: Pan-Arctic ice-wedge degradation in warming permafrost and its influence on tundra hydrology, *Nat. Geosci.*, 9, doi: 10.1038/ngeo2674, 2016.
- Luo, D., Wu, Q., Jin, H., Marchenko, S. S., Lü, L., and Gao, S.: Recent changes in the active layer thickness across the northern hemisphere, *Environ. Earth Sci.*, 75:555, doi:10.1007/s12665-015-5229-2, 2016.
- Marmy, A., Salzmann, N., Scherler, M., and Hauck, C.: Permafrost model sensitivity to seasonal climatic changes and
390 extreme events in mountainous regions, *Env. Res. Lett.*, 8, 035048, 2013.
- McCullagh, P. and Nelder, J.: *Generalized Linear Models*, 2nd edn, Chapman-Hall, London, 1989.
- McCune, B. and Keon, D.: Equations for potential annual direct incident radiation and heat load, *J. Veg. Sci.*, 13, 603–606, 2002.
- Melnikov, E. S., Leibman, M. O., Moskalenko, N. G., and Vasiliev, A. A.: Active-layer monitoring in the cryolithozone of
395 West Siberia, *Polar Geography*, 28, 267–285, 2004.
- Nakagawa, S. & Cuthill, I. C.: Effect size, confidence interval and statistical significance: a practical guide for biologists, *Biol. Rev.*, 82, 591–605, 2007.
- Oelke, C., Zhang, T., Serreze, M. C., and Armstrong, R. L.: Regional-scale modeling of soil freeze/thaw over the Arctic drainage basin, *J. Geophys. Res.*, 108, D10, 4314, doi:10.1029/2002JD002722, 2003.
- 400 Osterkamp, T. E.: Characteristics of the recent warming of permafrost in Alaska, *J. Geophys. Res.*, 112, F02S02, doi:10.1029/2006JF000578, 2007.
- Park, H., Walsh, J., Fedorov, A. N., Sherstiukov, A. B., Iijima, Y., and Ohata, T.: The influence of climate and hydrological variables on opposite anomaly in active-layer thickness between Eurasian and North American watersheds, *The Cryosphere*, 7, 631–645, 2013.
- 405 Peng, X., Zhang, T., Frauenfeld, O. W., Wang, K., Luo, D., Cao, B., Su, H., Jun, H., and Wu, Q.: Spatiotemporal changes in active layer thickness under contemporary and projected climate in the Northern Hemisphere, *J. Clim.*, 31, 251–266, 2018.
- R Core Team: R: A language and environment for statistical computing. R Foundation for Statistical Computing, Vienna, Austria, <https://www.r-project.org/>, 2015.
- 410 Romanovsky, V. E. and Osterkamp, T. E.: Effects of unfrozen water on heat and mass transport processes in the active layer and permafrost, *Permafrost Periglac.*, 11, 219–239, 2000.
- Romanovsky, V. E., Smith, S. L. and Christiansen, H. H.: Permafrost thermal state in the polar northern hemisphere during the International Polar Year 2007–2009: a synthesis, *Permafrost and Periglac.*, 21, 106–116, 2010.
- Romanovsky, V.E., Smith, S.L., Shiklomanov, N.I., Streletskiy, D.A., Isaksen, K., Kholodov, A.L., Christiansen, H.H.,
415 Drozdov, D.S., Malkova, G.V. and Marchenko, S.S.: Terrestrial Permafrost, *Bulletin of the American Meteorological Society*, 98, 147–149, 2017.
- Sheffield, J., Goteti, G., and Wood, E. F.: Development of a 50-year high-resolution global dataset of meteorological forcings for land surface modeling, *J. Clim.*, 19, 3088–3111, 2006.
- Shiklomanov, N. I.: Non-climatic factors and long-term, continental-scale changes in seasonally frozen ground. *Environ. Res. Lett.*, 7, 011003, doi:10.1088/1748-9326/7/1/011003, 2012.
- 420 Smith, M. W. and Riseborough, D. W.: Permafrost monitoring and detection of climate change, *Permafrost and Periglac.*, 7, 301–309, 1996.
- Smith, S. L., Wolfe, S. A., Riseborough, D. W., and Nixon, M.: Active-layer characteristics and summer climate indices, Mackenzie Valley, Northwest Territories, Canada, *Permafrost and Periglac.*, 20, 201–220, 2009.
- 425 Streletskiy, D. A., Anisimov, O., and Vasiliev, A.: Permafrost degradation, in: *Snow and ice-related hazards, risks and disasters*, Haerberli, W. and Whiteman, C. (Eds.), Elsevier, 303–344, 2015.



- Thuiller, W., Lafourcade, B., Engler, R., and Araújo, M. B.: BIOMOD – a platform for ensemble forecasting of species distribution, *Ecography*, 32, 369–373, 2009.
- 430 Vincent, W. F., Lemay, M., and Allard, M.: Arctic permafrost landscapes in transition: towards integrated Earth system approach, *Arctic Science* 3, 39–64, 2017.
- Westermann, S., Boike, J., Langer, M., Schuler, T. V., and Etzelmüller, B.: Modeling the impact of wintertime rain events on the thermal regime of permafrost, *The Cryosphere*, 5, 945–959, 2011.
- Westermann, S., Duguay, C. R., Grosse, G., and Kääh, A.: Remote sensing of permafrost and frozen ground, in: *Remote Sensing of the Cryosphere*, Tedesco, M. (ed.), Wiley, 307–344, 2015.
- 435 Woo, M.: *Permafrost Hydrology*, Springer-Verlag, Berlin Heidelberg, 2012.
- Wood, S. N.: Fast stable restricted maximum likelihood and marginal likelihood estimation of semiparametric generalized linear models, *J. R. Statist. Soc. B (Statistical Methodology)*, 73, 3–36, 2011.
- Wu, Q., Zhang, T., and Liu, Y.: Thermal state of the active layer and permafrost along the Qinghai-Xizang (Tibet) Railway from 2006 to 2010, *The Cryosphere*, 6, 607–612, 2012.
- 440 Zhang, T., Osterkamp, T. E., and Stamnes, K.: Effects of climate on the active layer and permafrost on the North Slope of Alaska, U.S.A., *Permafrost Periglac.*, 8, 45–67, 1997.
- Zhang, T., Chen, W., Smith, S. L., Riseborough, D. W., and Cihlar, J.: Soil temperature in Canada during the twentieth century: complex responses to atmospheric climate change, *J Geophys. Res.*, 110, D03112, doi:10.1029/2004JD004910, 2005.
- 445 Zhang, Y., Chen, W., and Cihlar, J.: A process-based model for quantifying the impact of climate change on permafrost thermal regimes, *J. Geophys. Res.*, 108, D22, 4695, doi:10.1029/2002JD003354, 2003.
- Zhang, Y., Sherstiukov, A. B., Qian, B., Kokelj, S. V., & Lantz, T. C.: Impacts of snow on soil temperature observed across the circumpolar north, *Environ. Res. Lett.*, 13, 044012, doi.org/10.1088/1748-9326/aab1e7, 2018.
- 450 Yi, Y., Kimball, J. S., Chen, R. H., Moghaddam, M., Reichle, R. H., Mishra, U., Zona, D., and Oechel, W. C.: Characterizing permafrost active layer dynamics and sensitivity to landscape spatial heterogeneity in Alaska, *The Cryosphere*, 12, 145–161, 2018.
- Yin, G., Niu, F., Lin, Z., Luo, J., and Liu, M.: Effects of local factors and climate on permafrost conditions and distribution in Beiluhe basin, Qinghai-Tibet Plateau, China, *Sci. Total Environ.*, 581-582, 472–485, 2017.



455 **Table 1: Adjusted coefficient of determination (R^2) and root mean square error (RMSE) between observed and predicted mean annual ground temperature (MAGT) and active-layer thickness (ALT) in calibration and evaluation (in brackets) datasets averaged over 100 permutations. GLM = generalized linear modelling, GAM = generalized additive modelling, GBM = generalized boosting method and RF = random forest.**

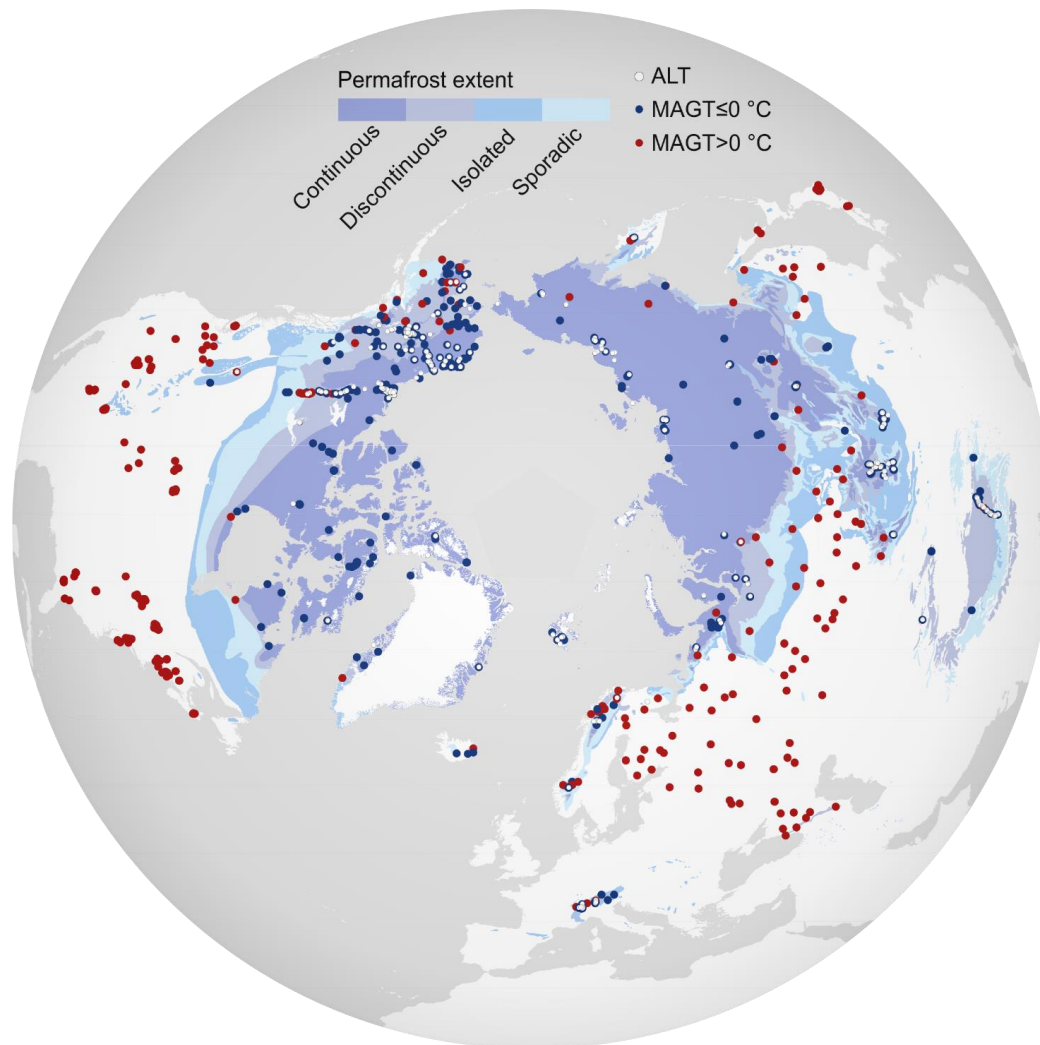
Method	MAGT ≤ 0 °C		MAGT > 0 °C		ALT	
	R^2	RMSE (°C)	R^2	RMSE (°C)	R^2	RMSE (cm)
GLM	0.86 (0.83)	1.24 (1.33)	0.95 (0.92)	1.20 (1.44)	0.65 (0.50)	80 (93)
GAM	0.88 (0.84)	1.17 (1.29)	0.95 (0.92)	1.18 (1.37)	0.70 (0.54)	74 (89)
GBM	0.93 (0.86)	0.88 (1.22)	0.97 (0.92)	0.91 (1.37)	0.84 (0.59)	55 (84)
RF	0.98 (0.87)	0.51 (1.17)	0.99 (0.93)	0.55 (1.27)	0.93 (0.62)	36 (82)
Average	0.91 (0.85)	0.95 (1.25)	0.96 (0.92)	0.96 (1.36)	0.78 (0.56)	61 (87)

460

Table 2: The effect size of individual predictors and their four-model averages (see Sect. 2.2 for abbreviations) in the original scale of the responses, °C for (mean annual ground temperature) MAGT and cm for active-layer thickness (ALT). The values are shaded with increasing blue (MAGT ≤ 0 °C), red (MAGT > 0 °C) and yellow (ALT) hues relative to the magnitude of the effect. GLM = generalized linear modelling, GAM = generalized additive modelling, GBM = generalized boosting method and RF = random forest. See Sect. 2.2 for predictor abbreviations.

465

	MAGT ≤ 0 °C (°C)					MAGT > 0 °C (°C)					ALT (cm)				
	GLM	GAM	GBM	RF	Avg	GLM	GAM	GBM	RF	Avg	GLM	GAM	GBM	RF	Avg
FDD	8.6	10.7	4.3	3.2	6.7	3.8	4.3	2.6	2.8	3.4	117	86	15	36	64
TDD	7.1	6.6	2.4	2.8	4.7	19.1	19.5	9.0	6.6	13.6	30	23	19	31	26
PrecipWater	1.6	2.6	4.3	3.0	2.9	4.8	3.6	0.2	0.7	2.3	372	249	28	74	181
PrecipSnow	4.4	4.4	0.1	0.2	2.3	0.8	1.4	0.3	0.5	0.8	195	146	44	94	120
SolarRad	2.6	2.5	0.2	0.3	1.4	2.0	2.3	0.9	1.6	1.7	135	193	178	139	161
CoarseSed	0.8	1.8	0.1	0.2	0.7	0.6	2.6	0.1	0.3	0.9	129	137	69	65	100
FineSed	0.5	0.7	0.2	0.4	0.4	0.6	0.7	0.1	0.1	0.4	17	20	7	9	13
SOC	0.5	0.4	0.3	0.8	0.5	1.7	1.4	0.1	0.6	0.9	121	129	30	28	77
NDVI	0.4	0.3	0.1	0.8	0.4	2.6	2.3	0.2	0.1	1.3	68	36	15	34	38



470 **Figure 1:** The observational network of the used mean annual ground temperature (MAGT) and active-layer thickness (ALT) across the circumpolar region. Blue symbols indicate the locations of boreholes where MAGT (averaged over the period 2000–2014) was at or below 0 °C and red symbols for those above 0 °C. White symbols depict the ALT measurements sites. The underlying permafrost zonation is from Brown et al. (2002).

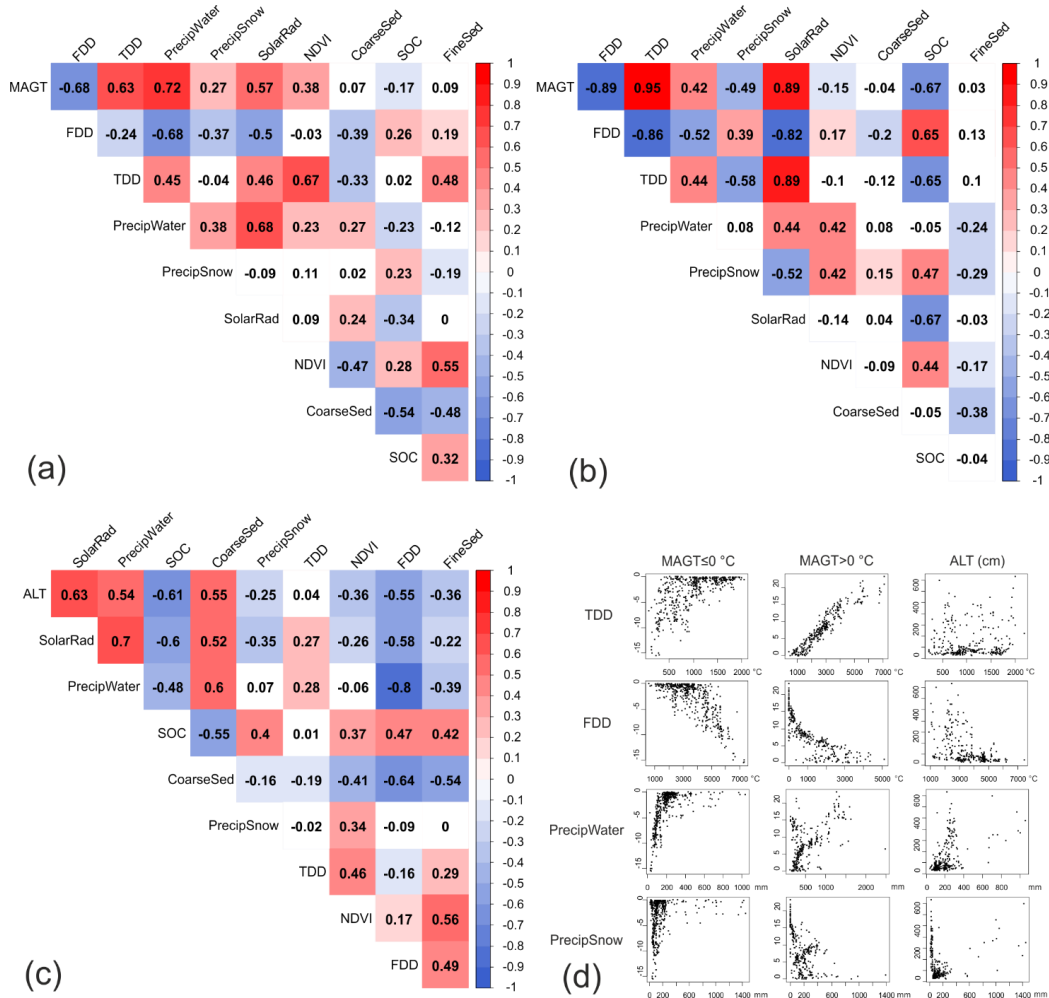


Figure 2: Spearman rank-order correlations between the predictor variables (see Sect. 2.2 for abbreviations) and MAGT_{≤0} °C (mean annual ground temperature) (a), MAGT_{>0} °C (b) and ALT (active-layer thickness) (c). Red hue stands for positive correlations, blue for negative, and white indicates non-significant ($p > 0.01$) correlations. Panel (d) shows MAGT and ALT observations plotted against the climatic predictors.

475

480

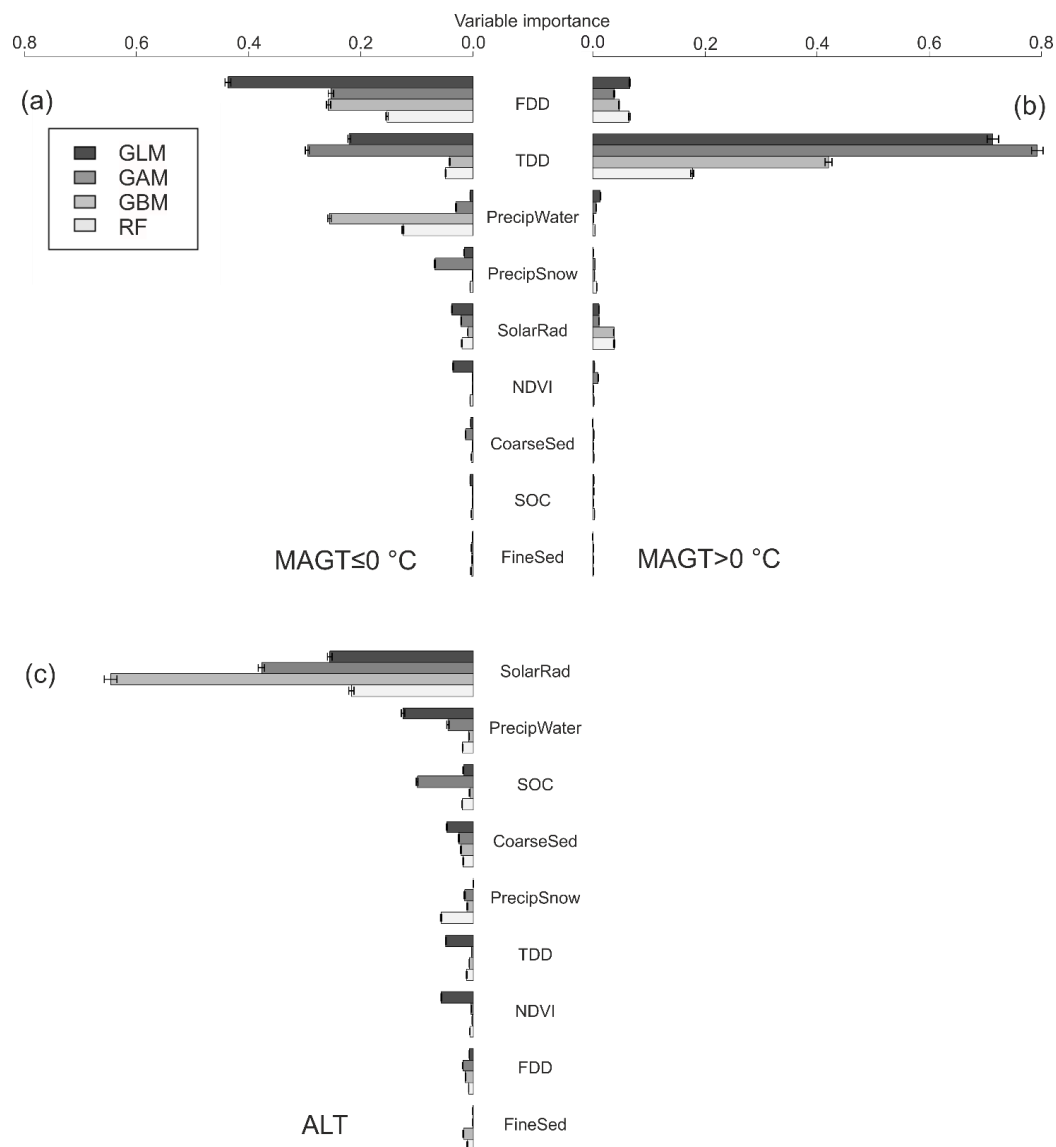
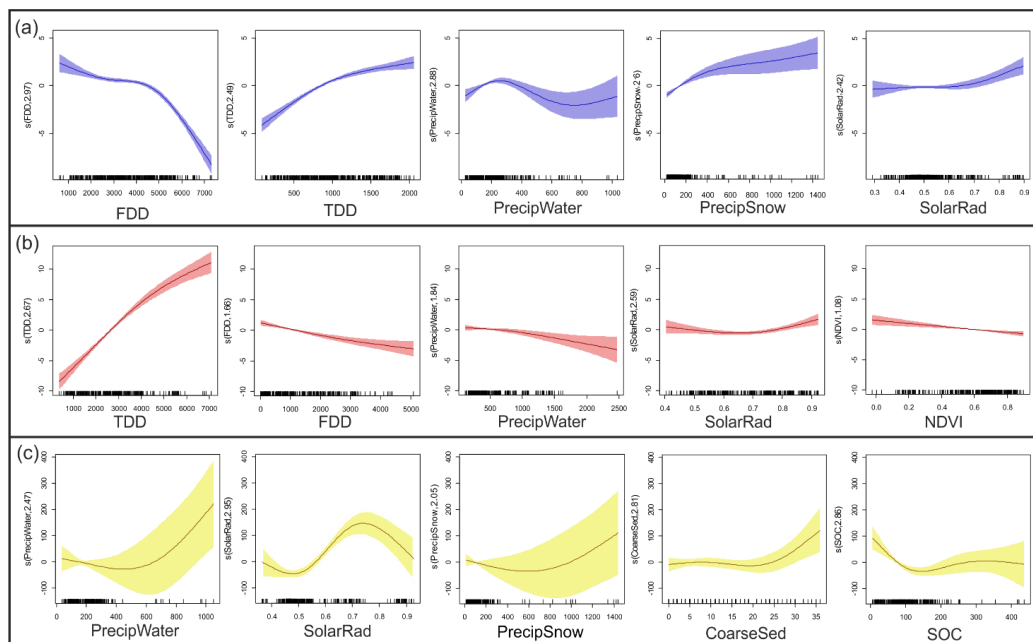


Figure 3: Variable importance values in MAGT_{≤0 °C} (mean annual ground temperature) (a) and MAGT_{>0 °C} (b) datasets arranged in the descending order of four-model average in MAGT_{≤0 °C} conditions, and for ALT (active-layer thickness) (c), arranged likewise based on ALT results. The whiskers depict 95 % confidence intervals (over 100 bootstrapping rounds). GLM = generalized linear modelling, GAM = generalized additive modelling, GBM = generalized boosting method and RF = random forest. See Sect. 2.2 for predictor abbreviations.

485



490

Figure 4: Response shapes of the five predictors with most contribution in $MAGT_{\leq 0}$ °C (mean annual ground temperature, blue curves), $MAGT_{> 0}$ °C (red curves) and ALT (active-layer thickness, yellow curves) datasets obtained from generalized additive modelling (GAM). Response shapes for the remaining predictors are illustrated in Figure S2. Predictors (see Sect. 2.2 for abbreviations) are presented in the descending order of their effect size in respective datasets. X-axis units appear in the original scale of the predictors. Y-axis displays partial residuals and labels the estimated degrees of freedom used in fitting the respective predictors to a response. Shaded areas depict 95 % confidence limits.